BENCHMARKING ADVANCED CONTROL ALGORITHMS FOR A LASER SCANNER SYSTEM

Andrzej W. Ordys*, Jakob Stoustrup** and Ian Smillie***

* Advanced Control Technology Club, Glasgow, UK.
** Dept. of Mathematics, Technical University of Denmark, Denmark.
*** Barr & Stroud Ltd. Glasgow.

Abstract : The paper describes tests performed on the laser scanner system to assess feasibility of modern control techniques in achieving a required performance in the trajectory following problem. The two methods tested are H_∞ and Predictive Control. The results are illustrated on a simulation example.

Keywords : modelling and simulation, predictive control, H_∞ control, systems with friction.

1. INTRODUCTION

1.1 Description of the scanner

Performance improvements in scanning devices offer the opportunity to cost-effectively build scanning systems that are simple, fast, accurate, compact, and capable of applications previously in the domain of other technologies. Traditional applications exist in industrial, commercial, medical, military, communications, and entertainment market. Newer applications are knocking at the door.

The function of the frame scan system is to sweep an optical beam across a focal plane array detector such that scene information can be gathered. This motion of the beam must meet system level interface requirements in regards to aperture, speed, and accuracy.

A galvanometric scanner is a form of electric motor in which the armature is restrained so that it can rotate only through angles of ±30° or less. A plane mirror with its surface parallel to the axis of rotation is rigidly mounted on the projecting shaft of the armature. The armature, mirror and mirror mount are collectively reffered to as the rotor.

For speed and accuracy the scanning system ought to posses high torque and high torque-to-inertia ratio. To meet these requirements, the scanning device designer must address the intertwined design and construction of the torque motor, mirror, suspension, and the position encoder.

The current moving-magnet scanners are build with rare-earth magnets that generate high torque without demagnetisation. They are designed for rigidity and structural integrity so that the scanner will not self destruct from fatigue. They also have the ability to dissipate heat generated in the stator coil so that the unit will not burn our. Thus, three critical design elements for a modern scanner are:

- an accurate, thermally stable mirror position detector,
- a rotor with a highly rigid armature, bearings, mirror and mirror mount;
- a stator drive coil with good thermal conductivity.

1.2 The control requirements specification

The operation of the scanner consist of oscillatory movements of the mirror, during which the optical information is gathered through the use of laser beam. For the purpose of this research, the optical part of the system is not considered. This research concerns only the control of the rotation of the mirror. The following parameters determine the performance of the system :

Scan angle : this determines the maximum field of view in object space. For contemporary designs the resulting mirror motion for the frame scanner falls in the range of ±5° to ±9° of displacement. An additional margin of ±3° is required for imaging calibration targets (thermal references) onto the array sensor. Thus, the rotational range of the frame scanner must provide ±12° of mechanical motion.

Scan rate : in order to be compatible with existing display standards, it is preferred that the frame scanner operates at the frequency of 50Hz (60Hz in USA)

Scan efficiency : this is directly related to the amount of time spent collecting scene information. Therefore, scan efficiency is defined as the ratio of linear scan time to scan period. At a scan rate of 50Hz a minimum scan efficiency of 80% is required to achieve current system level performance specifications.

Velocity non-linearity : linear operation of the frame scanner is critical to maintaining the image quality. By reducing the scan velocity non-linearity to the level of ±0.5% a special non-linearity compensation is no longer required. This can eliminate the dither noise in the detectors and therefore improve significantly the quality of images.

The control system requirements listed above can be illustrated as in Fig. 1. This figure presents a typical reference signal for the scanner system. The purpose of the control system is then to make the mirror angular position to follow this reference signal as tightly as possible, especially within the linear scan time.

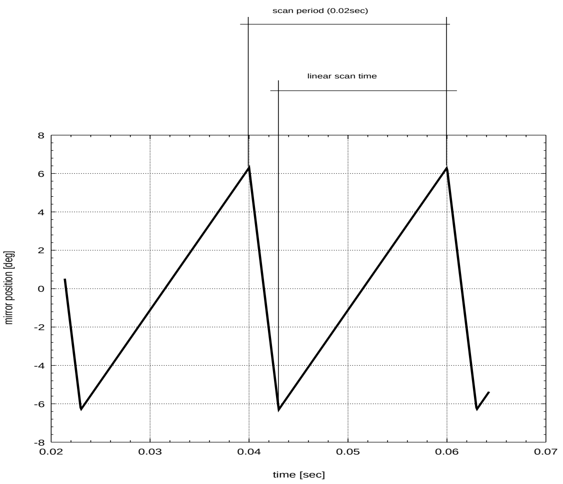

Fig. 1. The scanner reference signal.

2. MODELLING THE SCANNER

2.1 Main parts of the scanner system

Fig. 2 shows the MATRIXx representation of the overall block diagram of the scanner system. The system consists of :

- The reference signal generator (ramp generator). The reference signal is as depicted in Fig. 1.
- A digital controller which originally is a first order pole-zero compensator and is to be replaced by advanced control algorithms.
- A power amplifier block which includes the linear amplifier acting on the difference between the current demand from the controller and the actual motor current. The amplifier interface block limits the controller signal.
- Position sensor is a device which detects the mirror position and converts it into the electrical signal supplied to the controller.
- The mechanism which is the main part of the model and comprises the actuator and the representation for the scanner dynamics.

The actuator is described by the first order transfer function:

$$i_m = (sL + R)^{-1} \cdot \Delta V \tag{1}$$

where i_m is the motor current, ΔV represents the voltage supplied to the motor and is described by the equation :

$$\Delta V = V_m - \dot{\vartheta}_2 \cdot p_f \cdot K_b \tag{2}$$

In equation (2) V_m is the motor command (the signal from the power amplifier) and $\dot{\vartheta}_2$ is the mirror rate [rad/sec].

Finally, the electric torque produced is expressed by the equation :

$$T_e = i_m \cdot p_f \cdot K_t - c_g \tag{3}$$

Two coefficients in the torque equation represent nonlinear effects in the actuator. Those are :

profile (p_f) and cogging (c_g). Both profile and cogging are functions of the mirror position. L, R, K_b, K_t are constant parameters.

The load block represents a second order dynamics of the motor and the second order dynamics of the mirror. Those two are linked by the equation of torsional effect :

$$T_t = k_t(\vartheta_1 - \vartheta_2) \tag{4}$$

where ϑ_1 is the motor angle [rad] and ϑ_2 is the mirror angle [rad].

Friction and stiction are both included in the friction model.

3. ADVANCED CONTROLLER DESIGN AND COMPARISONS

3.1 Existing compensator

The pole zero compensator currently implemented in the scanner system is a first order digital controller described by the equation :

$$u_t = \left(b_1 z - b_2\right)^{-1}\left(a_1 z - a_2\right)(r_t - y_t) \tag{5}$$

where u_t is the control signal (current demand), r_t is the reference signal, and y_t is the position feedback signal.
The controller works with the sampling frequency 16 kHz.

3.2 H_∞ control

The approach taken was a two degrees of freedom design formulated in a standard problem set-up as a tracking problem with a reference model.

3.2.1 Reformulating the design specifications

Since H_∞ is in essence a frequency domain technique, time domain specifications has to be recast as frequency domain specifications. In the present case this meant that the L_∞ specification for the tracking error had to be transformed into a bandwidth specification for the transfer function from reference signal to tracking error. There is no one-to-one correspondence between L_∞ and bandwidth specifications, but a reasonable approach is to apply Fourier analysis to the reference signal, and require the bandwidth to include at least those harmonics that have amplitudes larger than or comparable to the maximally allowable error amplitude. In the present case, the bandwidth required using this approach was 1000 radians. This method turned out to work quite well for the scanner design.

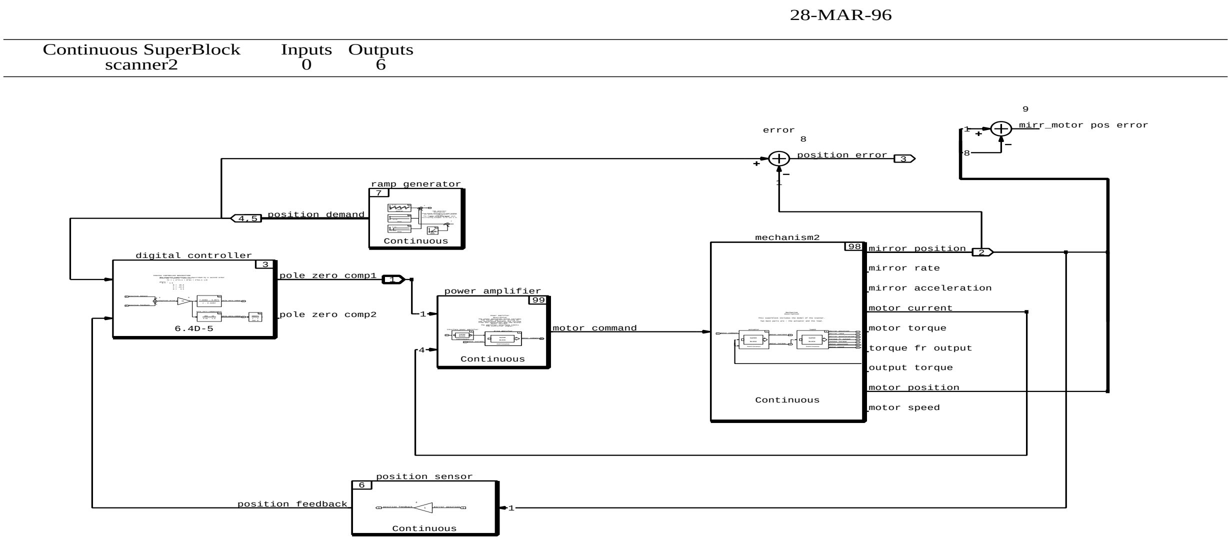

Fig.2. The MATRIXx representation of the scanner model.

3.2.2 Controller architecture

The laser scanner model was characterised by the following properties: strong nonlinearities, dominant oscillatory unstable modes, and an infinite zero structure. This calls for stability and performance issues to be addressed independently in order for the design to be robust. For this reason a two degrees of freedom architecture was chosen with a feedforward and a feedback block as shown in Fig. 3.

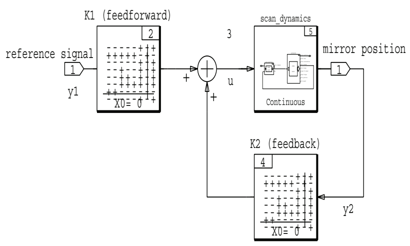

Fig. 3: TDOF architecture

The purpose of the feedback controller is to stabilise the system and provide as much bandwidth as is allowed by the non-linear dynamics without introducing nonminimum phase zeros inside the bandwidth specification, i.e. the feedback controller is not allowed to have unstable poles less than 1000 radians. The purpose of the feedforward controller is to provide the remaining bandwidth by amplifying fast components of the reference signal.

At this opportunity let it once again be mentioned that application of H_∞ control synthesis in itself does not guarantee robustness. Robustness in general is obtained only if designed for, and can be achieved also by other techniques than H_∞. In this case study it was chosen *not* to make a robust design for comparison to the other methods. Actually, the final design turned out to be reasonable robust with respect to parametric uncertainties, but that was related closer to the zero structure of the plant, than to the applied methods (parameter robustness is easier to obtain for a plant having no finite zeros).

3.2.3 Standard problem set-up and weight selection

To derive a standard problem set-up from the architecture in Fig. 3, it is required to:

1. introduce weightings
2. define "disturbance" signals
3. define "to-be-controlled" outputs

Ad 1: The most important weighting was of course the reference model, which is also well motivated since the reference signal was known in advance. For the architecture settled for it could also be relevant to have weightings representing actuator and sensor models, and possibly a noise model. However, these effects seemed to play minor roles, so only the reference weighting was included in the final design in order to keep the controller order down.

Ad 2: When introducing a weighting in front of the physical reference signal, the generating signal w_1 for the reference signal becomes the exogenous input. In addition to this signal, two fictitious noise signals w_2 and w_3 are added to the two measurement signals in order to prevent too large observer gains.

Ad 3: The output to be controlled is the difference between the desired output and the actual output, i.e. the tracking error. In addition to this signal z_1 we introduce a constant times the control signal u as the penalty signal z_2 to prohibit too large feedback gains.

The resulting standard problem is depicted in Fig. 4.

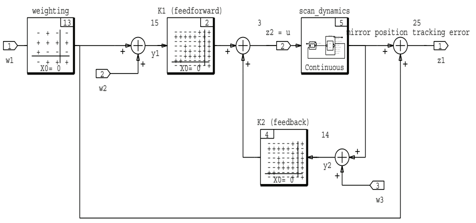

Fig. 4: Standard problem set-up.

The weighting function had to be chosen as a low pass filter with roll-off at 1000 radians. However, since the controller had to be implemented as a sampled data controller with a sampling of 100,000 radians, care had to be taken that the control gain would no be extremely high at that frequency. This meant that the weighting function had to roll of at least as a third order system, since the scanner system itself had a pole excess of five. Eventually, these considerations led to the selection of the weighting as a third order Bessel filter with Bessel angular frequency equal to 1000 radians.

The transfer function in Fig. 4 from $\begin{pmatrix} w_1 & w_2 & w_3 \end{pmatrix}^T$ to $\begin{pmatrix} z_1 & z_2 \end{pmatrix}^T$ is a linear fractional transformation with respect to the controller:

$$u(s) = \begin{pmatrix} K_1(s) & K_2(s) \end{pmatrix} \begin{pmatrix} y_1 \\ y_2 \end{pmatrix} \tag{6}$$

where $K_1(s)$ is the feedforward controller and $K_2(s)$ is the feedback controller in the following open loop standard problem configuration:

$$\begin{aligned}
\begin{pmatrix} \dot{x} \\ \dot{x}_W \end{pmatrix} &= \begin{pmatrix} A & 0 \\ 0 & A_W \end{pmatrix} \begin{pmatrix} x \\ x_W \end{pmatrix} + \begin{pmatrix} 0 & 0 & 0 \\ B_W & 0 & 0 \end{pmatrix} \begin{pmatrix} w_1 \\ w_2 \\ w_3 \end{pmatrix} + \begin{pmatrix} B \\ 0 \end{pmatrix} u \\
\begin{pmatrix} z_1 \\ z_2 \end{pmatrix} &= \begin{pmatrix} C & -C_W \\ 0 & 0 \end{pmatrix} \begin{pmatrix} x \\ x_W \end{pmatrix} + \begin{pmatrix} -D_W & 0 & 0 \\ 0 & 0 & 0 \end{pmatrix} \begin{pmatrix} w_1 \\ w_2 \\ w_3 \end{pmatrix} + \begin{pmatrix} D \\ \rho I \end{pmatrix} u \\
\begin{pmatrix} y_1 \\ y_2 \end{pmatrix} &= \begin{pmatrix} 0 & C_W \\ C & 0 \end{pmatrix} \begin{pmatrix} x \\ x_W \end{pmatrix} + \begin{pmatrix} D_W & \lambda I & 0 \\ 0 & 0 & \lambda I \end{pmatrix} \begin{pmatrix} w_1 \\ w_2 \\ w_3 \end{pmatrix} + \begin{pmatrix} 0 \\ D \end{pmatrix} u
\end{aligned} \tag{7}$$

Here, $G(s) = \begin{pmatrix} A & B \\ C & D \end{pmatrix}$ and $W(s) = \begin{pmatrix} A_W & B_W \\ C_W & D_W \end{pmatrix}$ are the plant and weighting transfer functions respectively. ρ and λ are scalar parameters with the dual purpose of regularising the plant as required for toolbox computations, and of controlling filtering and feedback gains as mentioned above.

3.2.4 Computing the controller

Mainly two commercial toolboxes offer H_∞ optimisation: i.e. Robust Control Toolbox and the $\mu-$tools toolbox. Both toolboxes are available both for MATLAB and for MATRIXx.

None of these two toolboxes were useful without some customisation. Entering the data as in model described in Section 2 directly did not result in any controllers for any value of γ. The reason for this was that both toolboxes regarded the system to be nonstabilisable for numerical reasons, whereas the model really turned out to be controllable for structural reasons at a closer look. The reason for these problems were not obvious since the model seemed quite "innocent". A partly explanation is probably that the system had a strongly non-collocated actuator-sensor structure. This tends to generate systems with very ill-conditioned controllability matrices.

As a means to overcome these numerical problems, a numerically balanced version of the model was computed. Since also the built-in balancing tools broke down (because the system was not well balanced!!) an ad hoc procedure was established, based on geometric methods (the details are omitted due to space limitations). This balanced model was further reduced from a fifth order model to a fourth order model in order to bound the resulting controller order. The toolbox methods will always generate controllers with the order of the plant plus that of the weightings. Low controller orders is a basic virtue of designers. However, in the present case-study this aspect was not so much required from an implementational point of view, but rather because the simulation tools could not handle high order controllers. As an example, using the built-in conversion from state space to transfer funtion representations in MATRIX-X, meant a qualitative change to the outcome of the simulation, i.e. a change from stability to instability, in spite of the fact that the very same controller was applied!

The next issue to address was discretisation, since the controller should be implemented in a sampled-data realisation. Again the built-in default did not work very well. Both in MATLAB and MATRIX-X, the default choice is the Tustin approximation. For the H_∞ controller the Tustin approximation worked at low frequencies only. This meant that the resulting controller was not even stabilising. Instead the discretisation was carried out using the prewarp algorithm, which is based on a bilinear transform, using one fifth of the sampling frequency for the prewarp.

Following this algorithm, an H_∞ controller was derived which worked quite well for the linearised model. The error signal, i.e. the difference between the command signal and the output of the linearised model using the sampled-data TDOF H_∞ controller is shown in Fig. 5.

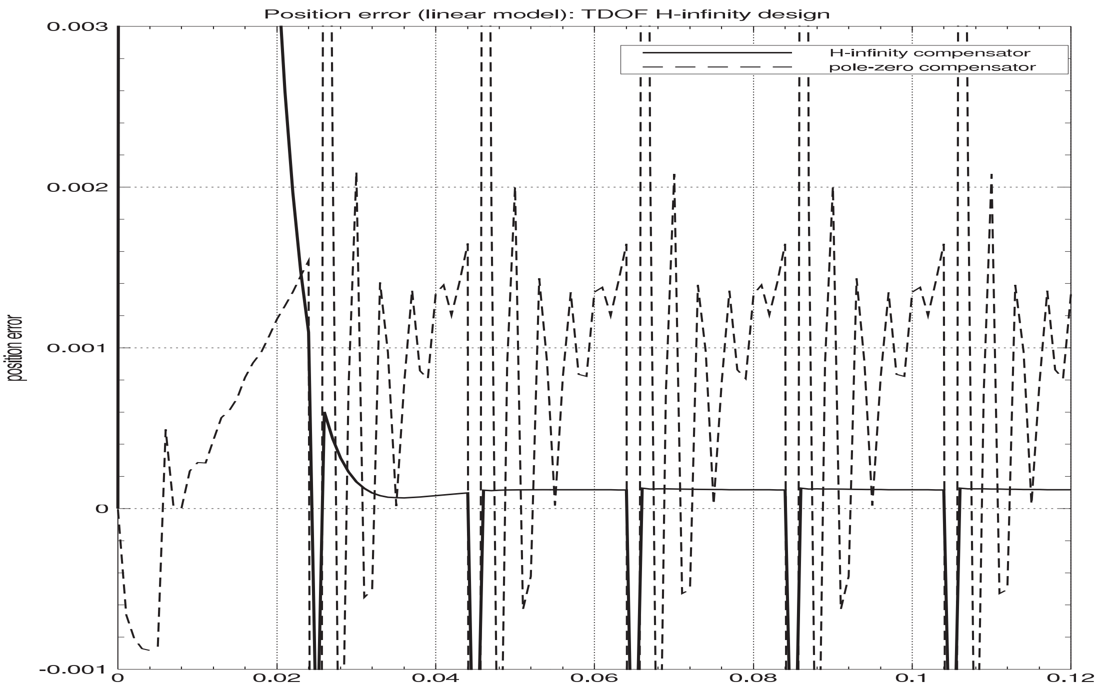

Fig. 5: TDOF H_∞ controller for linearised model.

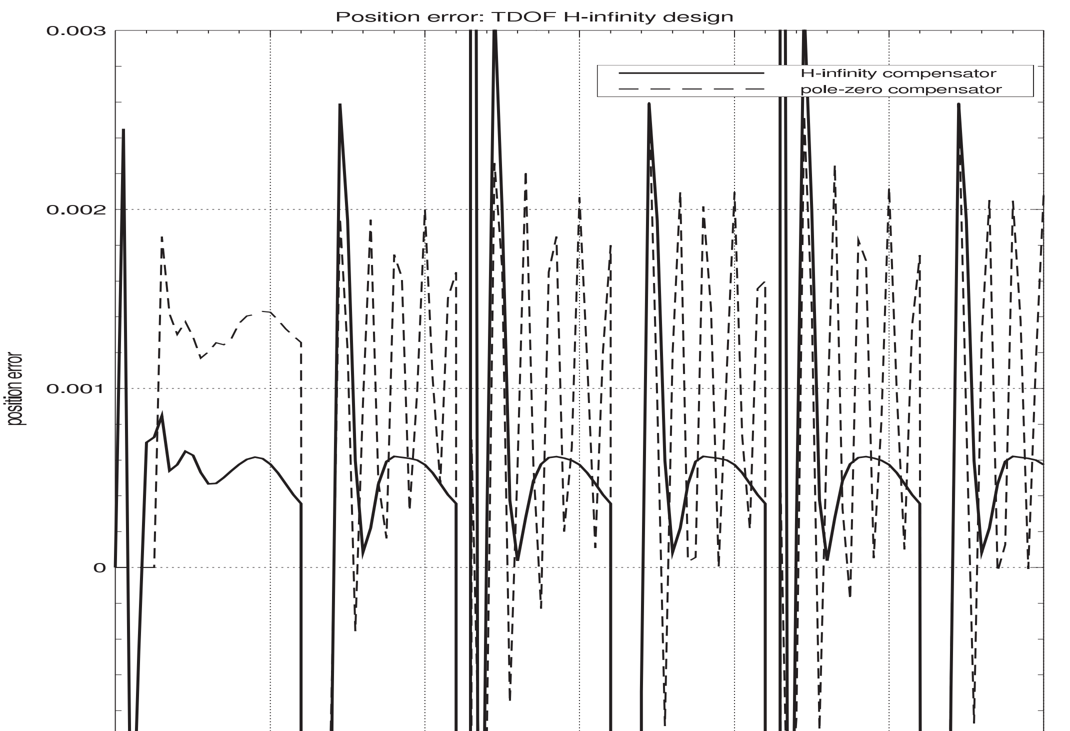

Fig. 6: TDOF H_∞ controller for nonlinear model.

When this TDOF controller was applied to the non-linear model, it did not work very well. It managed to stabilise the non-linear model, but it had a very poor performance. From the simulations it was very clear what happened: each time the mirror turned its directions, it got stuck because of the static friction. The recipe was obvious as well: the low frequency gains had to be increased. However, this could not easily be built into the design procedure. An inverting-the-plant procedure which would yield the largest gain producable by the toolbox would still be a factor of 10^3 too low. And introducing a robust stability/nominal performance (mixed sensitivity) concept, would actually have made everything worse (smaller LF gains). On the other hand, trying to work with alternate linearised models obtained by linearising near the stiction phenomena would also not work, since the HF components would disappear.

An ad hoc approach was taken by introducing the LF high gains manually, simply by adding a first order high gain LP transfer function to the feedback part of the controller. This immediately overcame the problem, and the design specifications were met in the first iteration. The result of this design can be seen in Fig. 6, which compares the resulting error from the existing pole-zero compensator with the TDOF H_∞ controller. Note that the error from the H_∞ controller does not have high frequency oscillations, and that it stays well within a 0.001 boundary during 85% of each period.

The resulting controller was of the same order as the standard problem, i.e. its state space has 5-1=4 dimensions from the reduced order model, 3 dimensions from the Bessel filter, 1 dimension from the first order LP gain, so the total controller order was 8. With some effort this could be reduced a little, but not substantially.

3.3 Generalized predictive control

3.3.1 Introduction to the algorithm

The design of predictive control algorithm requires some initial manipulations on the scanner system model. Firstly, the nonlinear model must be linearised. This has been performed using a standard MATRIXx function. Secondly, the resulting model,which is expressed in continuous time, must be discretised, as the GPC controller utilises a discrete time model. Several methods of discretisation are available in MATRIXx. From those, a trapezoidal (Tustin) method was selected as this one is consistant with other operations performed on discrete superblocks within MATRIXx package. However, when applying the Tustin discretisation, the resulting discrete time model usually has direct through terms, i.e. algebraic coonections between input and output signals. The Generalised Predictive Control algorithm must be modified to handle this situation.

The system considered is described by linear discrete time state space equations in the form :

$$\begin{aligned} x_{t+1} &= Ax_t + B_1 u_t \\ y_t &= Cx_t + D_1 u_t \end{aligned} \tag{8}$$

where :

x_t - vector of state variables,

u_t - vector of inputs which are manipulated control signals,

y_t - vector of output variables,

A, B, C, D - constant matrices (D defines the direct through terms)

In order to simplify the derivation of the optimal control, it is mathematically convenient to rearrange the state equations (8), by extending the state vector to include the control signals as follows :

$$\chi_{t+1} = \tilde{A} \cdot \chi_t + \tilde{B} \cdot \Delta u_{t+1} \tag{9}$$

$$y_t = \tilde{D} \cdot \chi_t \tag{10}$$

where :

$$\chi_t = \begin{bmatrix} x_t \\ u_t \end{bmatrix}, \tag{11}$$

$$\tilde{A} = \begin{bmatrix} A & B \\ O & I \end{bmatrix}, \quad \tilde{B} = \begin{bmatrix} O \\ I \end{bmatrix}, \quad \tilde{D} = \begin{bmatrix} C & D \end{bmatrix} \tag{12}$$

Having obtained the extended state equations of the system, the derivation of the GPC controller can be performed as in a standard case. The k-step ahead output prediction becomes:

$$y_{t+k} = \tilde{D}\chi_{t+k} = \tilde{D}\tilde{A}^k \chi_t + \sum_{j=1}^{k} \tilde{D}\tilde{A}^{k-j}\tilde{B}\Delta u_{t+j} \tag{13}$$

If the prediction is performed for different time horizons (from 1 to N) the result may be collected in a block vector $Y_{t,N}$ consisting of output predictions for j=1,...N. When the system variables are unconstrained there exists an analytical solution of the problem in the form :

$$U_{t,N}^{opt} = \left(G_1^T G_1 + \lambda \cdot I\right)^{-1} G_1^T \left[R_{t,N} - \Phi\tilde{A}\chi_t\right] \tag{14}$$

where :

$$G_1 = \begin{bmatrix} \tilde{D}\tilde{B} & & & \\ \tilde{D}\tilde{A}\tilde{B} & & O & \\ \vdots & & & \\ \tilde{D}\tilde{A}^N\tilde{B} & \tilde{D}\tilde{A}^{N-1}\tilde{B} & \cdots & \tilde{D}\tilde{B} \end{bmatrix} \tag{15}$$

$R_{t,N}$ - vector of the future values of the reference signal,

The dimension of the G_1 matrix and the required matrix inversion in (14), can be reduced by setting a control horizon $N_u < N$. After N_u steps into the future the control increment is set to zero. Thus the last $N - N_u$ rows of G_1 may be deleted, since in this case they make no contribution to the output prediction. N_u represents a tuning parameter in GPC, which may be used to shape the control performance and to stabilise non-minimum phase or unstable plants.

Because a receding horizon strategy is employed only the first element of the predicted optimal controls vector $U_{t,N}$ is actually applied to the system. At each sampling instance new measurement information becomes available and $U_{t,N}$ is updated according to (14). If the future reference signal matches exactly the predicted free response summed with a known future disturbance component, then the current control increment will be zero.

3.3.2 Implementation of GPC

The algorithm described in previous section has been tested on the nonlinear scanner model. This appeared to be a difficult task.

Firstly, the linearised version of the scanner model, which has been utilised in the Predictive Control design is unstable. The Predictive Controller must stabilise the system. Note that the Generalised Predictive Controller presented in this paper is capable of stabilising an unstable scanner model. This is not an obvoius feature of all predictive controllers.

Secondly, an interesting feature of the analysed model is that it requires a vigorous control action for stabilisation. therefore, even a minimal costing on control signals in the performance index causes instability of the whole system.

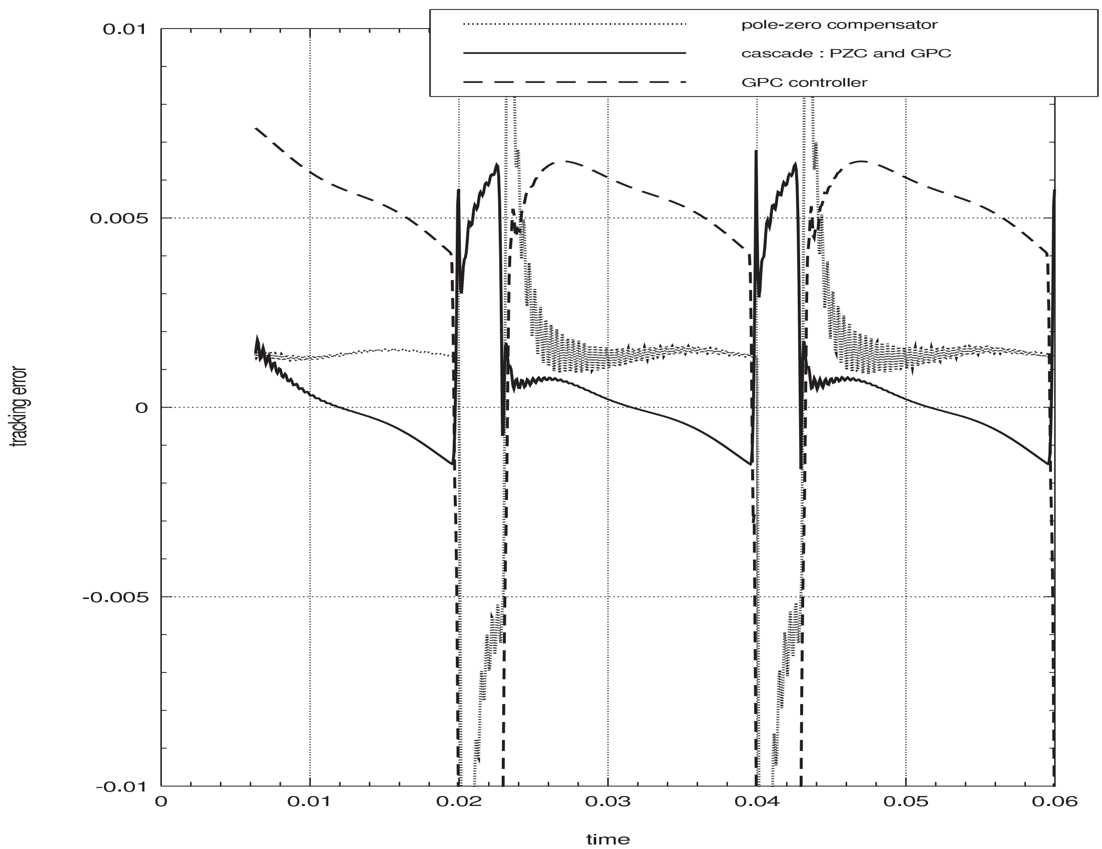

Fig. 7. Comparison of scanning errors for : pole-zero compensator, Generalised Predictive Controller, and cascade of pole-zero compensator and GPC.

Replacing the existing pole-zero compensator with a Generalized Predictive Controller resulted in much smaller overshoots at the beginning and at the end of the scanning period. However, the error during the rest of the scanning period was not much better than with the pole-zero compensator (see Fig. 7).

Another approach tried in this implementation experiment was to leave the existing pole-zero compensator and to apply Generalised Predictive Controller in an outer loop, providing set point value for the pole-zero compensator (cascade control). This approach is justified by the fact that the pole-zero compensator provides stabilisation of the scanner system. then the role of the GPC would be to optimise the performance. For this exercise the scanner and the pole-zero compensator were linearised and discretised together and the resulting model was used in the GPC design.

The results of the above described experiments are depicted in Fig. 7. It is easy to notice that the last of the described approaches provides a superior performance of the system. In both cases of implementation of Generalised Predictive Control, the immediate result was elimination of overshoots at the beginning and at the end of the scanning period. This of course can help to improve the scan efficiency. However, it was difficult to achieve a noticeable reduction of the scanning error. To obtain better results it would probably be necessary to come back to the modelling exercise and construct a more exact linear model of the scanner.

4. CONCLUSIONS

The paper presents an exercise on feasibility of modern control techniques, namely H_∞ and Model Based Predictive Control, to provide a required performance in the trajectory following problem for the laser scanner system. The scanner system poses serious difficulties to the control design due to its strong nonlinearity (caused mainly by the static friction) and the highly undamped instability of the linearised model. After some careful tuning, both H_∞ and Generalized Predictive Control were capable of successfully controlling the system. Particular features of the compared algorithms are as follows:

H_∞ provides lower value of the scanning error during the linear scanning period than the GPC algorithm. GPC is capable of removing overshoots at the beginning and at the end of the scanning period, which poses difficulties to the H_∞ algorithm.

The H_∞ controller was easier to tune than the GPC.

ACKNOWLEDGEMENTS

This paper was originated by a case study project realised by Advanced Control Technology Club, Glasgow for Barr and Stroud Ltd.

REFERENCES

Ludwiszewski A., Standard module approach to scanning requirements for second generation airborne FLIRs, source not known, 1994

Armstrong-Helouvry B., P. Dupont and C. Canudas de Wit, A survey of models, analysis tools and compensation methods for the control of machines with friction, Automatica, Vol 30, No.7, 1994

Canudas de Wit C., H. Olsson, K.J. Astrom and P. Lischinsky, A new model for control of systems with friction, IEEE Transactions on Automatic Control, Vol. 40, No. 3, March 1995

Marshall G.F., Scanner refinements inspire new users, Laser Focus World, June 1994

Ordys A.W. and D.W. Clarke, A state-spce description of GPC controllers, International Journal of Systems Science, Vol. 23, No.2, 1993

Limebeer D.J.N., E.M. Kasenally, and J.D. Perkins, On the design of robust two degrees of freedom controllers, Automatica, Vol. 29, No. 1. 1993

Grimble M.J., Minimization of a Combined H_∞ and LQG cost function for a two-degrees-of-freedom control design, Automatica, Vol. 25, No.4, 1989